Supplement of Atmos. Chem. Phys., 17, 11605–11621, 2017
https://doi.org/10.5194/acp-17-11605-2017-supplement

Atmospheric Chemistry and Physics
Open Access
EGU

Supplement of

Secondary organic aerosol from atmospheric photooxidation of indole

J. Montoya-Aguilera et al.

Correspondence to: Sergey A. Nizkorodov (nizkorod@uci.edu)

Contents

S1. Wall loss corrections

The wall loss correction was done by assuming a first-order particle size independent loss of particle mass concentration (*PM*)

$$\frac{dPM}{dt} = \text{Source(t)} - \text{Loss(t)} = \text{Source(t)} - k_w \times PM\ , \quad \text{(S1)}$$

where the *Source*(*t*) and *Loss*(*t*) are time dependent production and removal rates for the particles. The effective first-order rate constant k_w = 0.00090 min^{-1} was determined in a separate experiment in which indole SOA was produced, the lamps were turned off, and mass concentration of SOA was followed with the SMPS for 10 hours without collecting SOA on filters. Using the known k_w, we could determine *Source*(*t*) from the actual measured PM concentration in every experiment.

$$\text{Source(t)} = \frac{dPM}{dt} + k_w \times PM\ , \quad \text{(S2)}$$

The corrected PM concentration (i.e. the hypothetical PM concentration that would be achieved if the wall loss was absent) was calculated from:

$$PM_{corrected}\text{(t)} = \text{PM(t} = 0) + \int_0^t Source(t)dt, \quad \text{(S3)}$$

The integration of data was carried out numerically in Excel. Figure 3 in the main text shows a representative result of the wall loss correction.

S2. PTR-ToF-MS measurements of indole and volatile products of indole photooxidation

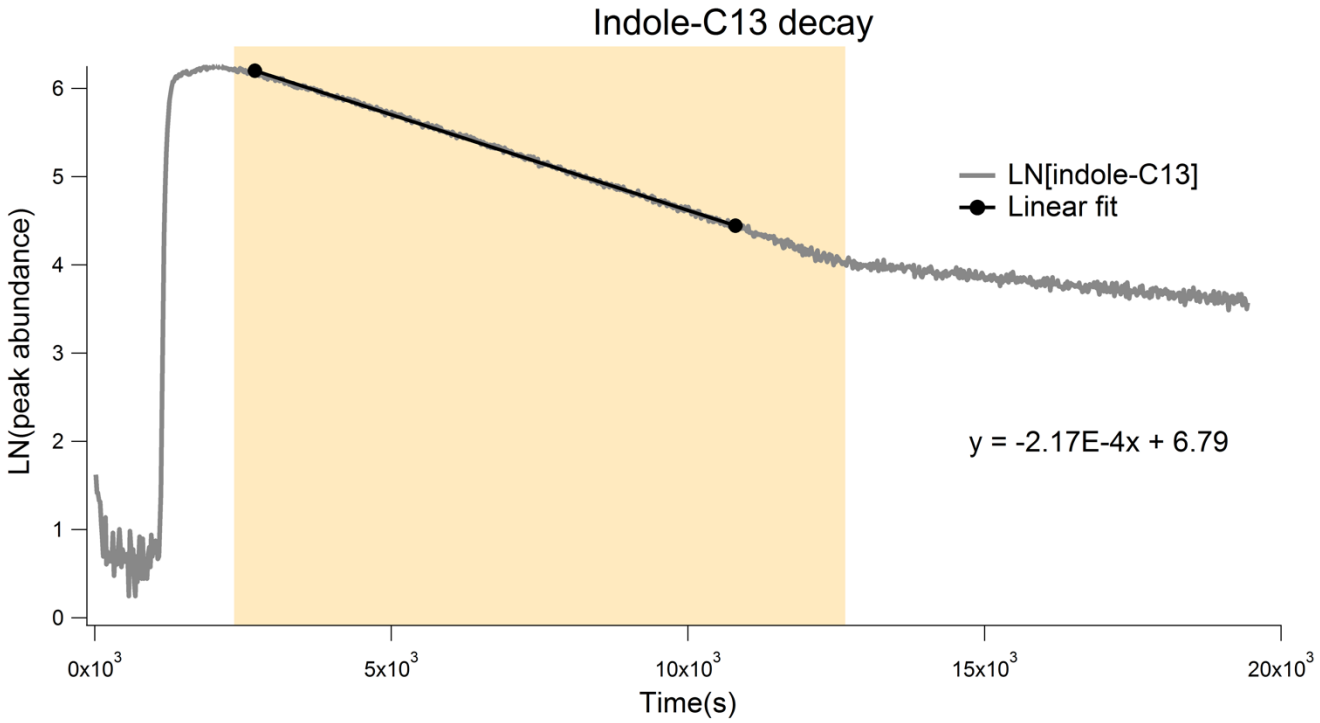

Figure S2.1: Estimating the OH concentration in the chamber

The OH concentration was estimated from the rate of loss of indole (measured using the ^{13}C isotopic ion of protonated indole observed at *m/z* 119). The slope translates into [OH] ~1.4×10^{6} molec cm^{-3}. The break in the time dependence corresponds to switching off the UV lights and simultaneously starting collecting the samples. The shaded region denotes the time when the chamber lamps were on.

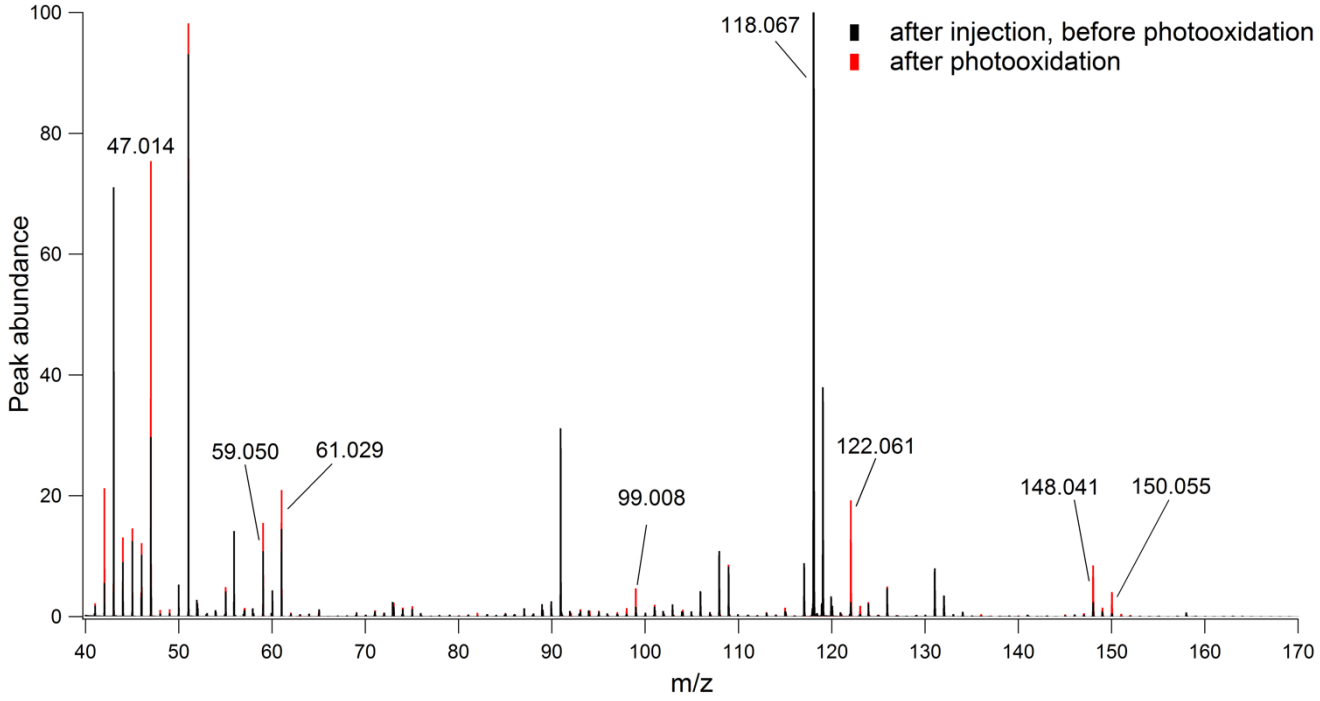

Figure S2.2: Mass spectra of the chamber VOC compounds before and after photooxidation of indole

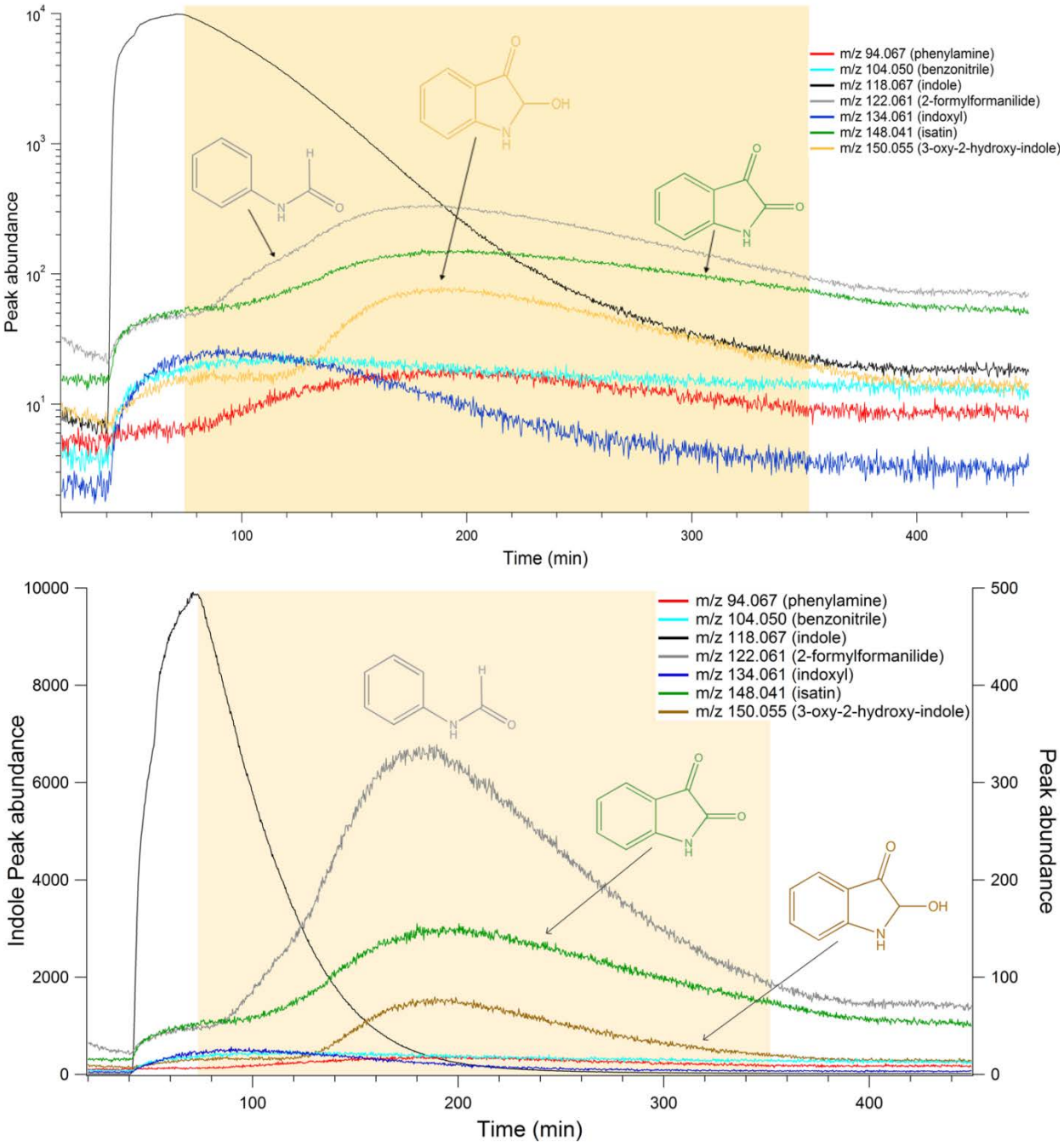

Figure S2.3: Time-dependent signals of ions that were produced and then removed

Shaded region denotes the time when the chamber lamps were on. The top panel shows data on the log scale and the bottom panel shows data on the linear scale. Note that segments of the sampling line for PTR-ToF-MS were not heated, and the observed time dependence may be complicated by the adsorption equilibria on the sampling

tube surfaces. For example, the unusual time dependence for *m/z* 150.055 (3-oxy-2-hydroxy-indole, drawn in yellow) and *m/z* 148.041 (isatin, drawn in green) was reproducible, and likely resulted from delayed passage of these compounds through the sampling lines. However, the time dependence makes it possible to sort observed compounds into ones produced by the UV radiation from the chamber lamps, and ones that are less affected (or not affected at all) by the UV radiation. This particular plot shows compounds that clearly went up when the UV lamps were on; their removal at later time is from secondary photooxidation.

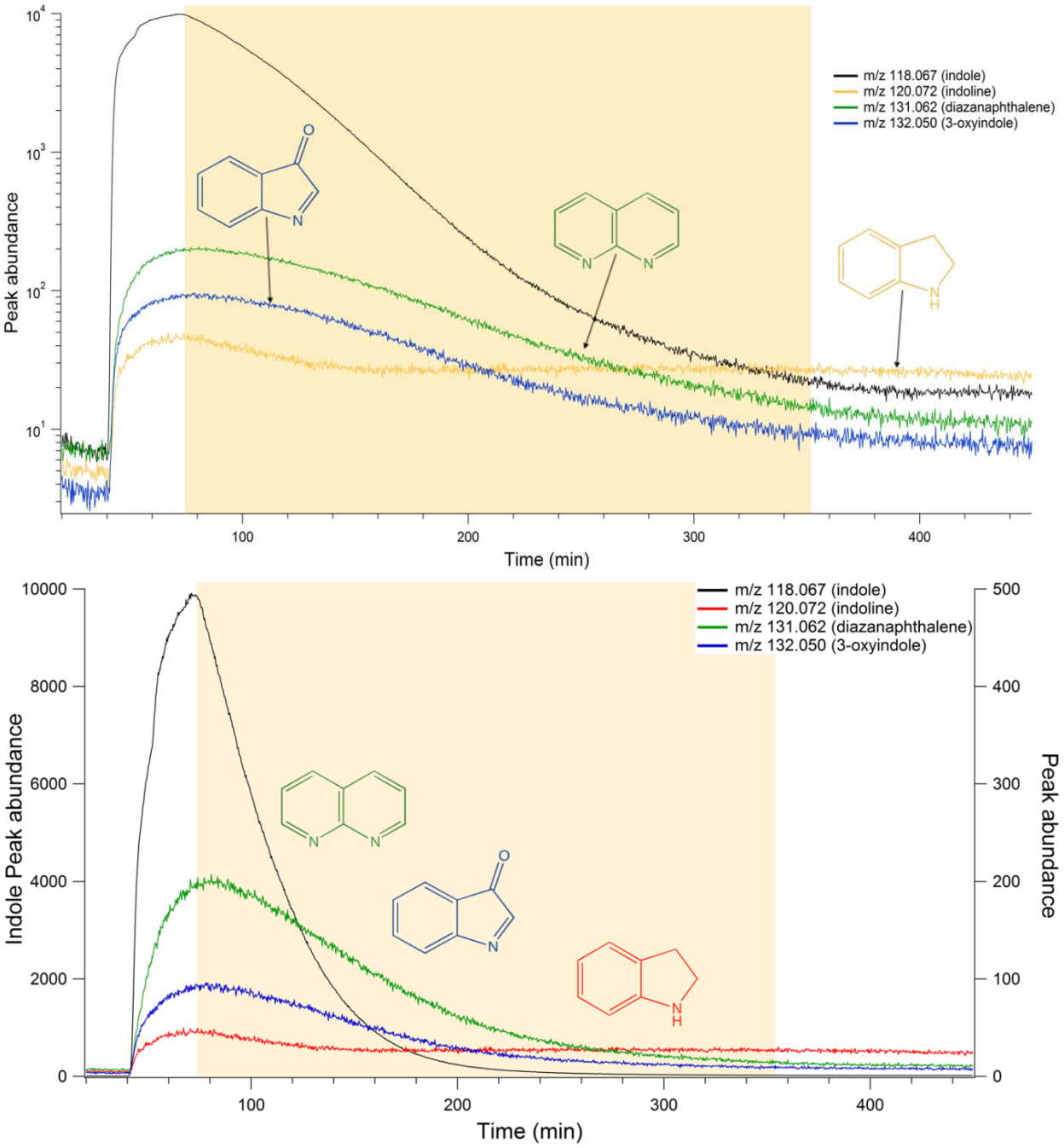

Figure S2.4: Time-dependent signals of ions that were removed during photooxidation

Shaded region denotes the time when the chamber lamps were on. The top panel shows data on the log scale and the bottom panel shows data on the linear scale. Indoline and diazanaphthalene were likely present in the indole sample to begin with, as impurities.

Table S2. Summary of assigned PTR-ToF-MS peaks

Calibrated m/z	Exact *m/z*	Ion Formula	Neutral Formula	Possible Assignment	Behavior
44.014	44.0131	CH_2NO^+	HOCN	cyanic acid	produced
45.034	45.0335	$C_2H_5O^+$	C_2H_4O	acetaldehyde	produced
46.029	46.0287	CH_4NO^+	CH_3NO	nitrosomethane	produced
47.014	47.0128	$CH_3O_2^+$	HCOOH	formic acid	produced
59.050	59.0491	$C_3H_7O^+$	C_3H_6O	acetone	produced
61.029	61.0284	$C_2H_5O_2^+$	$C_2H_4O_2$	acetic acid	produced
90.950	90.9477	$FeO_2H_3^+$	$H_2O{\cdot}FeO$	produced in ion source	
94.067	94.0651	$C_6H_8N^+$	C_6H_7N	phenylamine (aniline)	produced then removed
98.026	98.0237	$C_4H_4NO_2^+$	$C_4H_3NO_2$	maleimide	produced
99.008	99.0077	$C_4H_3O_3^+$	$C_4H_2O_3$	maleic anhydride	produced
104.050	104.0495	$C_7H_6N^+$	C_6H_5CN	benzonitrile	produced then removed
118.067	118.0651	$C_8H_8N^+$	C_8H_7N	indole	removed
120.072	120.0808	$C_8H_{10}N^+$	C_8H_9N	indoline (impurity)	removed
122.061	122.0600	$C_7H_8NO^+$	C_7H_7NO	2-formylformanilide	produced then removed
131.062	131.0604	$C_8H_7N_2^+$	$C_8N_6N_2$	diazanaphthalene (impurity)	removed
132.050	132.0444	$C_8H_6NO^+$	C_8H_5NO	3-oxyindole	removed
134.061	134.0600	$C_8H_8NO^+$	C_8H_7NO	indoxyl, 3-oxindole	produced then removed
148.041	148.0393	$C_8H_6NO_2^+$	$C_8H_5NO_2$	isatin	produced then removed
150.055	150.0550	$C_8H_8NO_2^+$	$C_8H_7NO_2$	3-oxy-2-hydroxy-indole	produced then removed

S3. N/C ratio in indole SOA compounds

Reactions that involve oxidation and oligomerization of indole without loss of C or N atoms should conserve the N/C ratio at the value of 1/8 (= 0.125), the initial value in indole. Loss and gain of N atoms should result in a large decrease and increase in the N/C ratio, respectively. Loss and gain of C atoms should result in a small increase and decrease in the N/C ratio, respectively. All of these processes are clearly happening in the photooxidation of indole although the N/C conserving processes are clearly dominant.

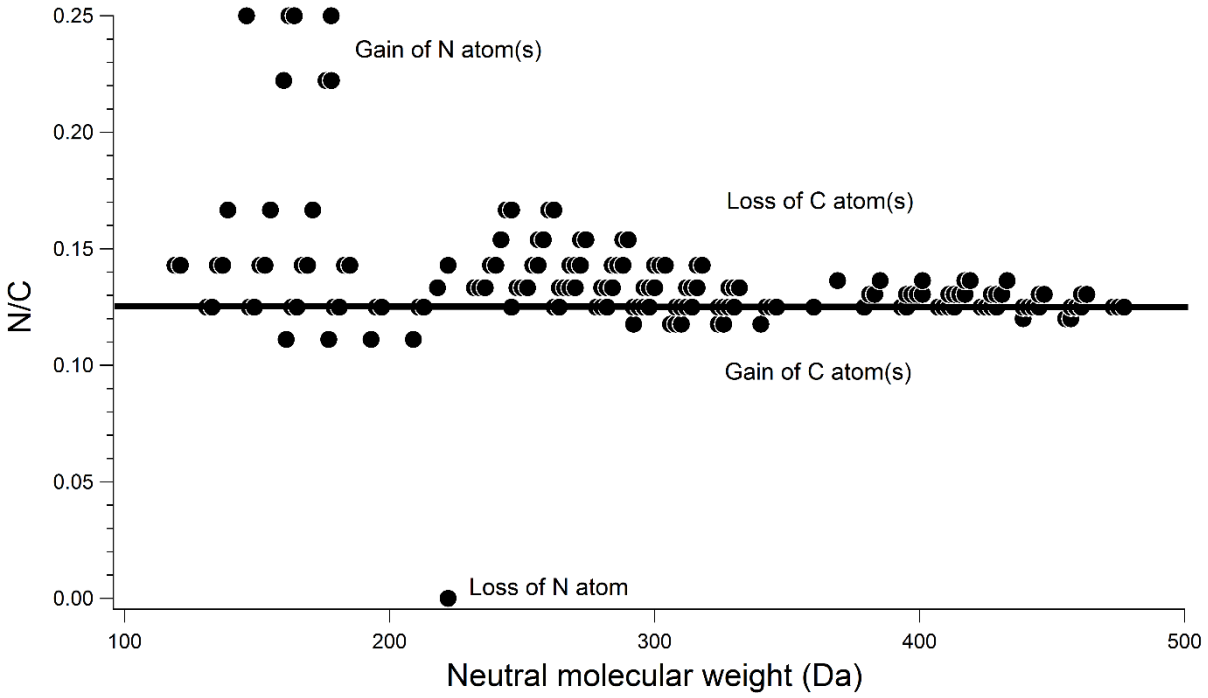

Figure S3: The N/C ratio of indole SOA compounds

The thick horizontal line corresponds to the N/C ratio in indole.

S4. Spatial distribution of gas-phase indole concentrations in SoCAB

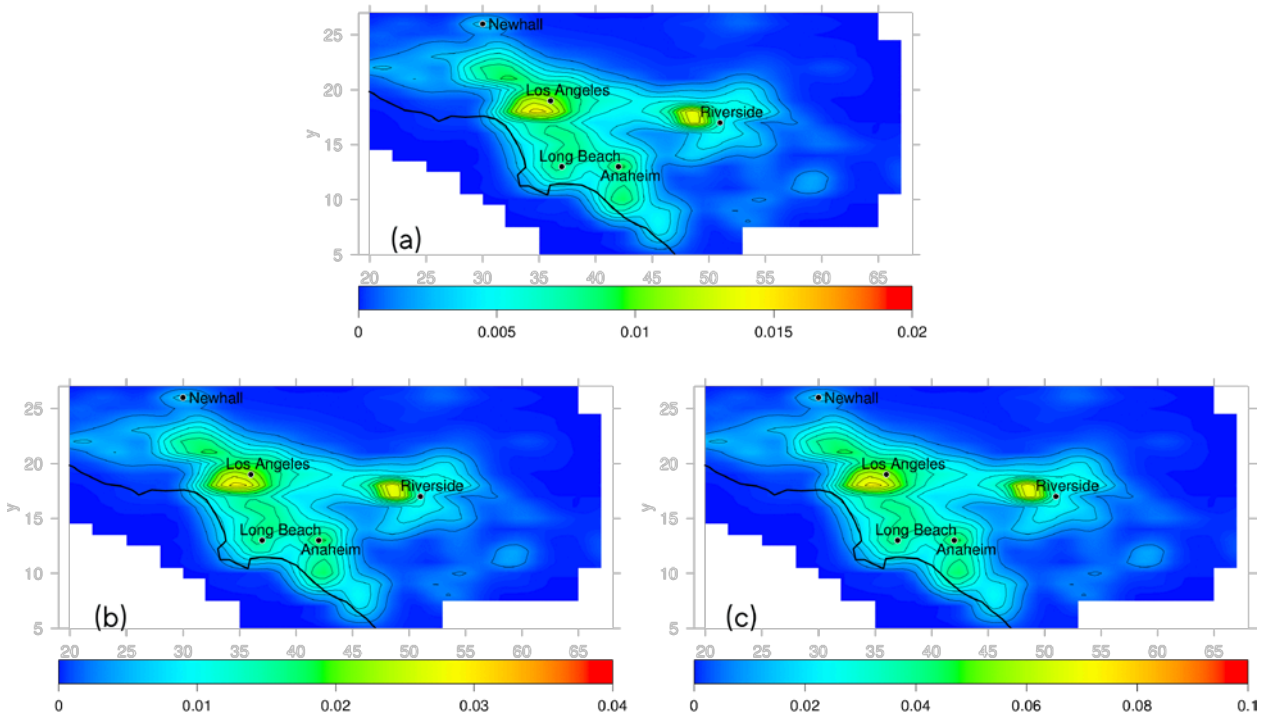

Figure S4: The 24-hour average gas-phase indole concentrations

The indole mixing ratios in ppbv are shown in the low emission scenario (a), medium emissions scenario (b), and high emission scenario (c).

S5. Diurnal profile of gas-phase indole concentrations in SoCAB

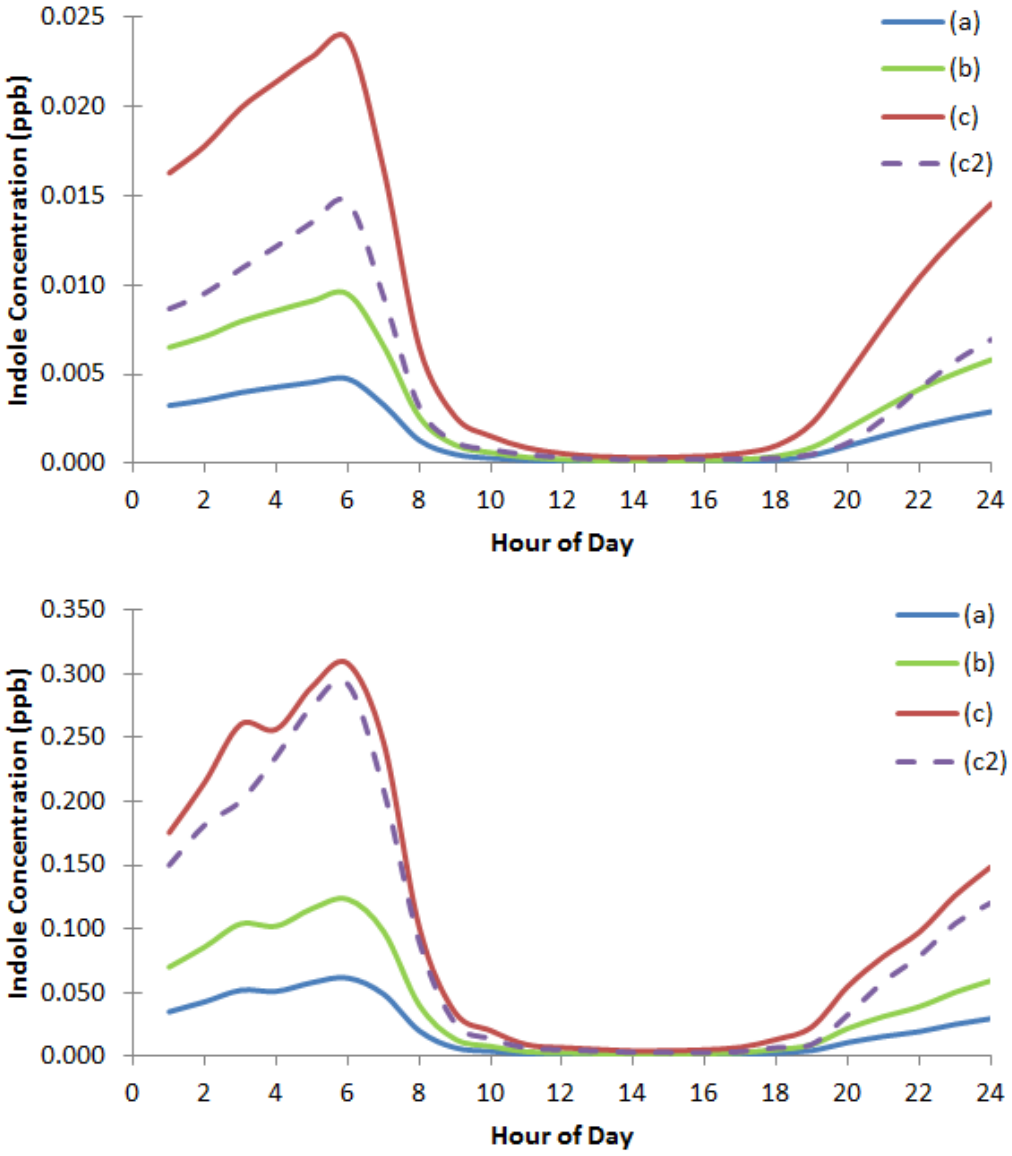

Figure S5: Gas-phase indole concentrations

The indole mixing ratios in ppbv are shown for the low emissions scenario (a), medium emissions scenario (b), and high emissions scenario (c). In addition, trace (c2) shows mixing ratios in the high emissions scenario with indole oxidation via reaction with NO_3 included in the model. Domain wide average concentrations are shown in the top panel and domain maximum concentrations are shown in the bottom panel.

S6. Diurnal profile of SOA concentrations in SoCAB

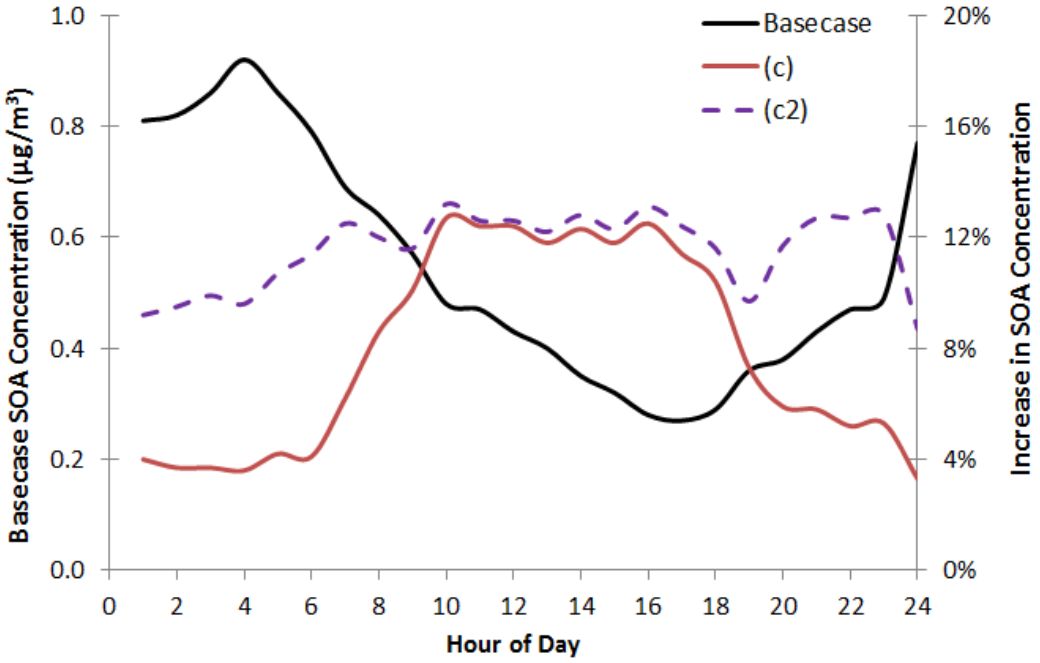

Figure S6: Domain wide average SOA concentrations

The base case mass concentration of SOA is shown in black line referenced to the left axis. Also shown is the percent increase in the domain wide average SOA concentrations (right axis) due to indole SOA in the high emissions scenario (c), and high emissions scenario with indole oxidation via reaction with NO_3 included in the model (c2). The daytime concentrations are not significantly affected by NO_3 but the nighttime concentrations increase.